Noninvasive Monitoring of Local Drug Release Using X-ray Computed Tomography: Optimization and *In Vitro*/*In Vivo* Validation

AGATA SZYMANSKI-EXNER,[1] NICHOLAS T. STOWE,[2] KYLE SALEM,[1] ROEE LAZEBNIK,[1] JOHN R. HAAGA,[3] DAVID L. WILSON,[1] JINMING GAO[1,3]

[1]Department of Biomedical Engineering, Case Western Reserve University, 10900 Euclid Avenue, Cleveland, Ohio 44106

[2]Department of Surgery, Case Western Reserve University School of Medicine, Cleveland, Ohio 44106

[3]Department of Radiology, University Hospitals of Cleveland, Cleveland, Ohio 44106

Received 30 May 2002; accepted 24 August 2002

ABSTRACT: *In vivo* release profiles of drug-loaded biodegradable implants were noninvasively monitored and characterized using X-ray computed tomography (CT). The imaging method was adapted and optimized to quantitatively examine the release of an active agent from a model cylindrical PLGA device (the millirod) into rabbit livers over 48 h. Iohexol, a CT contrast agent, served as a model drug; optimization of CT acquisition parameters yielded a sensitivity of 0.21 mg/mL (or 95 μg iodine/mL) for this agent. *In vitro* validation of the method was carried out by tracking release of iohexol in gelatin gel phantoms. *In vivo* release in rabbit livers was characterized through quantitative analysis of CT images and compared with UV-Vis analysis of the explanted devices at three implantation times. After correction for respiratory motion, CT analysis correlates well with the extracted iohexol data at all time points. The percent error between the actual and experimental image data was below 10%. This study demonstrates the potential of using computed tomography to noninvasively quantify the rate of agent release from controlled delivery devices *in vivo*. © 2003 Wiley-Liss, Inc. and the American Pharmaceutical Association J Pharm Sci 92:289–296, 2003

Keywords: noninvasive monitoring; drug delivery devices; X-ray CT; iohexol

INTRODUCTION

Monitoring the principal characteristics (e.g., release kinetics) of a drug delivery system *in vivo* under unperturbed physiological conditions is important for the rational design and development of a device with optimal drug dosage, release rate, and duration. These parameters are essential for achieving a safe and sufficient local therapy in a specific tissue environment. Typical clinical pharmacokinetic studies gather the needed data from the collection of blood or tissue samples, and/or removed implants.[1] The release profile of a particular drug delivery method is then indirectly determined through the analysis of plasma and tissue drug concentrations using high-performance liquid chromatography (HPLC), high resolution mass spectrometry, or atomic absorption spectrometry (AAS). These procedures are invasive, and require the sacrifice of many animals and, in addition, data analysis may be complicated by variability between animals.

To overcome these limitations, significant research effort has been focused on the development of noninvasive imaging techniques to characterize

Correspondence to: Jinming Gao (Telephone: 216-368-1083; Fax: 216-368-4969; E-mail: jmg23@po.cwru.edu)

Journal of Pharmaceutical Sciences, Vol. 92, 289–296 (2003)

the release kinetics of drugs in the target tissue *in vivo*.[2,3] Gamma-emission imaging, positron-emission tomography (PET), and magnetic resonance imaging (MRI) are three modalities that have been used in clinical pharmacokinetic studies.[4–6] Limitations of these methods are relatively low spatial resolution (5 and 10 mm for clinical gamma imaging and PET, respectively) and low sensitivity for MRI imaging.[4,7] In this study, we used clinical X-ray computed tomography as an imaging modality for tracking the characteristic behavior of an interstitial drug delivery device *in vivo*. Compared to other noninvasive imaging techniques, CT provides outstanding spatial resolution ($0.3 \times 0.3 \times 0.5$ mm^3), speed and high sensitivity without the need to radiolabel the drugs.

The physical basis of CT contrast originates from the different abilities of materials to attenuate the X-ray photons in a beam of radiation. For a CT contrast agent such as iohexol, the attenuation is mostly caused by photoelectric absorption of primary photons by the heavy element, in this case iodine ($Z = 53$). The CT contrast of different materials can be characterized and quantified by their linear attenuation coefficients (μ, unit: cm^{-1}) or mass attenuation coefficients (μ_m, cm^2/g). The difference in attenuation coefficients provides the physical basis of CT contrast of various agents over background tissue.[8–10] For example, at 80 keV the values of μ_m for carbon and iodine are 0.16 and 3.51 cm^2/g, respectively.[11] The linear relationship between attenuation (leading to image contrast) and agent concentration is the basis of our functional utilization of this imaging technique.[8–10]

Here, we report on the development and application of the CT method in examining the release kinetics of an agent from a polymer implant into rabbit livers. The model drug delivery device used in this study consists of a biodegradable polymer matrix entrapping a CT contrast agent, iohexol (Omnipaque®). The purpose for such a model system is twofold: it allows for accurate assessment of the noninvasive CT monitoring method in pharmacokinetic studies while providing valuable insight regarding the local drug release kinetics in the liver.

The central hypothesis behind this research is that noninvasive monitoring of local drug delivery using CT will lead to a better understanding of the drug pharmacokinetics *in vivo* for device optimization that cannot be normally observed with *in vitro* or *ex-vivo* analysis. We propose that the combination of X-ray CT and image analysis techniques may provide an alternative direct method for the evaluation of the transport of drugs containing a heavy element (such as iodine or platinum) from localized, controlled release devices. In this study, we have optimized the image acquisition technique and imaging parameters to maximize the sensitivity and resolution, established image analysis procedures for quantitative measurement, and validated the method in a gelatin model system as well as in rabbit livers *in vivo*.

MATERIALS AND METHODS

Materials

Poly(D,L-lactide-*co*-glycolide) (PLGA, lactide: glycolide = 1:1, 0.65 dL/g inherent viscosity) was purchased from Birmingham Polymers, Inc. (Birmingham, AL). Iohexol (Omnipaque®, MW 821.14, melting point 174–180°C, 46.36% iodine content) was purchased from Nycomed Amersham Imaging (Oslo, Norway) and poly(vinyl alcohol) (PVA, 13,000–23,000 Da molecular weight, 87–89% hydrolyzed) was purchased from Aldrich (Milwaukee, WI). D(+)-Glucose was purchased from Fluka (Milwaukee, WI). Phosphate-buffered saline (PBS), methylene chloride, and gelatin (275 bloom) were obtained from Fisher Scientific (Pittsburgh, PA). Teflon tubes were purchased from McMaster–Carr Supply Company (Cleveland, OH). New Zealand White rabbits were obtained from Covance (Princeton, NJ).

Implant Fabrication and *In Vitro* Characterization

Millirod implants were fabricated according to a previously established compression-heat molding procedure.[12] Briefly, PLGA microspheres (~4 μm) were mixed with iohexol powder to form a uniform mixture, and D(+)-glucose was added to the mixtures to expedite the rate of release. The homogeneously mixed powder was placed in a mold and compressed at 4.6×10^6 Pa at 90°C for 2 h. The resulting cylindrical millirods have an average diameter of 1.65 mm and a loading density of 10% iohexol with 30% glucose (w/w).

The *in vitro* release of iohexol from the millirods was measured in PBS buffer (pH 7.4) using a procedure reported previously.[12] Typically, segments of millirods (~8 mm in length) were submerged in 10 mL PBS and placed in an orbital shaker (New Brunswick Scientific, model C24) at

37°C and 100 rpm agitation. At each sampling point, the millirod was removed from the vial and placed into 10 mL of fresh PBS. The retained sample was analyzed using a UV-Vis spectrophotometer (Hitachi, model U-3210). The Beer-Lambert law was used to calculate the iohexol concentration based on a previously determined extinction coefficient [34.8 mL/(mg · cm)] at the maximum absorption wavelength (245 nm) of iohexol. The average amount of iohexol remaining in the implants with time was calculated from this data and was standardized to the initial loading of iohexol.

Optimization of CT Image Acquisition Parameters and Sensitivity Measurement

All studies were performed with a multislice CT scanner (MX 8000^{TM}, Philips Medical Systems, Highland Heights, OH) at University Hospitals of Cleveland. Gelatin gels containing iohexol concentrations from 0.01 to 10 mg/mL were used as imaging phantoms to evaluate the sensitivity of detection under various image acquisition conditions. The gels were produced by dissolving 1 g of gelatin in a 10 mL solution of different iohexol concentrations. The influence of the CT parameters such as peak kilovoltage of the X-ray beam (kVp), current-time (mAs), and slice thickness were investigated. These parameters were examined systematically, with each set of data being analyzed and optimized before proceeding to the next study. The other parameters were kept constant: helical scan at 0.5 mm pitch, 1.5-s rotation time, B filter, high resolution, 160 mm field of view (FOV) and 512×512 pixel matrix.

CT image analysis was performed with ImageJ (NIH, http://rsb.info.nih.gov/ij/). For the optimization studies, the middle four slices (or the middle two in the 2.5-mm case) were analyzed to account for the partial volume effect, where the data from the top and bottom edges of the plate may be averaged with the air, and incorrect pixel values would be obtained. The analysis consisted of selecting a circular region of interest (ROI) of 120–125 pixels and determining the values along the perimeter. The average and standard deviation of the CT intensity in Hounsfield Units (HU) of these pixels were calculated. Next, the average CT intensity was plotted versus iohexol concentration and the slope of the line was determined. This slope was then used to convert the standard deviation in Hounsfield Units (σ_{HU}) to standard deviation in concentration (σ_C). Then, the sensitivity was calculated by taking the ratio of the noise to the concentration (σ_C/C). The value of σ_C/C was then plotted versus the iohexol concentration and a power curve ($y = ax^b$) was fitted to each set of data to estimate the sensitivity cutoff. We defined the concentration at which the signal is equal to noise (σ_C/C = 1) as the sensitivity limit of iohexol detection by CT for each set of parameters.

In Vitro Validation of CT Method

Gelatin gel phantoms were initially used as a tissue-mimicking environment to determine the accuracy of the CT method in monitoring the release of iohexol from polymer millirods. Implants were inserted periodically over 6 days into 10% gelatin gels formed in 50-mL Falcon tubes, and iohexol was allowed to be released from the millirod and diffuse into the matrix. The tissue phantoms were imaged using optimized parameters, and the implants were immediately removed from the gels after the CT scan. The iohexol remaining in the implants was extracted into PBS over 6 days and analyzed by UV-Vis spectrophotometry. The average CT intensity in each implant was determined from image analysis of circular ROIs (five-pixel diameter) averaged along the length of each implant. A background value for the polymer was subtracted from the average ROI measurement to obtain the signal from iohexol.

The release of iohexol was assessed by calculating the contrast change with time on the images and correlating this value to the UV-Vis measurement of extracted iohexol. These data were standardized to the values at $t = 0$. For the CT data, the average intensity in HU for the millirods scanned immediately after implantation into gels ($t = 0$) was used to calculate the percentage of release at other time points. For the comparable chemical analysis, the same millirods were removed from the gels, and the extracted iohexol concentration was measured with UV-Vis and used as the standardization value for the other time points.

In Vivo Validation and CT Monitoring of Iohexol Release

Animal procedures followed an approved protocol by the Institutional Animal Care and Use

Committee at CWRU. Male New Zealand white rabbits (3–3.5 kg) were used in these studies. The animals were anesthetized with xylazine (5 mg/kg), acepromazine (2 mg/kg), and ketamine (50 mg/kg). The right and medial liver lobes were exposed through a small incision in the midsection, and the capsule was perforated with an 18-gauge needle. A section of the millirod (6–8 mm) was implanted into each lobe. After implantation, a small piece of fat was removed from the animal and sutured on top of the implant to seal the site.

Imaging parameters obtained from the optimization studies (600 mAs, 120 kVp, 1-mm slice thickness) were used to monitor the *in vivo* release of iohexol. The rabbits remained sedated with incremental administration of ketamine (50 mg/kg) during the scans. Each rabbit was positioned in the CT scanner so that the scan plane was approximately perpendicular to the long axis of the millirod. The animals were imaged independently at three time points (1, 4, and 24 h) using the optimized scan parameters. The rabbits were then sacrificed and the scan was repeated. The millirods were removed and iohexol was extracted into PBS and analyzed with UV-Vis spectrometry. The CT images were processed as described below.

Image Processing and Analysis of Iohexol Release *In Vivo*

A three-dimensional registration method was utilized to spatially align serial CT volumes. A detailed description of this method was described previously.[13–15] This approach uses line paths and point landmarks to obtain volume registration. After registration, the image volume was resliced so that the orientation of the slices was exactly perpendicular to long axis of the millirod. Based on phantom simulations of manual localization error and millirod orientation typical of our *in vivo* experiments, we predicted a voxel displacement registration error of less than 0.5 mm. The new image slices were analyzed with ImageJ for the relative change of intensity within the implanted rod. The average concentration of iohexol remaining within the implant was estimated by calculating average pixel values in circular ROIs within the millirod body (five-pixel diameter) and subtracting the average base polymer attenuation level (in gelatin) from the average data. The conversion value of 8.46 HU/(mg/mL) obtained from gelatin studies was used to calculate the iohexol concentration.

Correction Factor for Respiratory Motion

Several experiments were carried out to examine the effect of motion artifacts on the accuracy of the concentration measurements obtained from image data analysis. We suspected that the lengthy 1.5-s rotation time used for minimizing noise and maximizing sensitivity during image acquisition might result in motion blur and artifact that would limit the quantitative concentration measurement. To examine the extent of motion artifact, we compared CT measurements of iohexol concentration in studies with movement (live animal) and without movement (following animal sacrifice) at three time points. A correction factor was calculated as the slope of a linear fit between data without motion versus with respiratory motion. This factor was applied to all other *in vivo* concentration measurements to correct motion artifact in living, breathing animals.

RESULTS

Implant Fabrication and *In Vitro* Release Studies

The fabrication process yielded reproducible implants with a homogeneous iohexol distribution. Based on the implant volume, concentration of iohexol was calculated to be 154 ± 11 mg/mL ($n = 5$). Figure 1 shows the release profile of iohexol from PLGA implants in PBS. The time at which 50% of the active agent was released

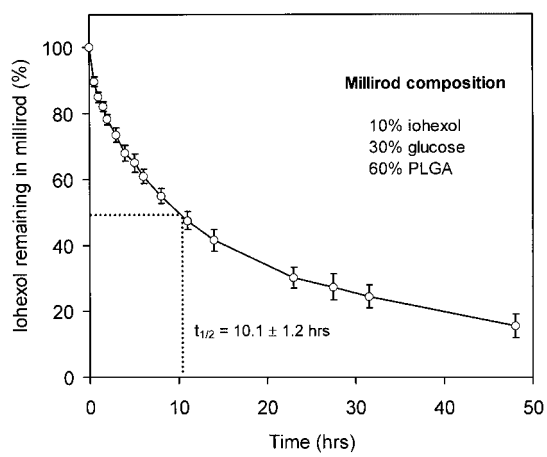

Figure 1. *In vitro* release of iohexol from polymer millirods into PBS buffer at 37°C. The cumulative release is illustrated as the percent iohexol remaining in the implant over time. The error bars were calculated from five samples.

from the matrix ($t_{1/2}$) was determined by linear extrapolation and found to be 10.1 ± 1.2 h. Over 90% of the agent was released after 60 h (data not shown).

CT Optimization and Sensitivity of Detection

Table 1 summarizes the results from the CT optimization and sensitivity studies. We found that increasing the current-time, peak kilovoltage, and/or the slice thickness increases the sensitivity and improves the limit of iohexol detection. We discuss these findings in detail below. Quantitative data analysis of the gelatin phantoms indicates that the sensitivity ranges from 0.18 to 0.30 mg/mL iohexol for the evaluated parameters. The sensitivity curves for these two extremes are shown in Figure 2. The lowest concentration of iohexol that exceeds the quantum noise is 0.18 mg/mL. However, because the slice thickness needs to be 2.5 mm to achieve this limit, this set of parameters compromised the resolution for our application and will not be considered. The lowest sensitivity attained with a practical set of parameters is 0.21 mg iohexol/mL at 600 mAs, 120 kVp, and 1-mm slice thickness. These parameters were chosen as the most favorable image acquisition conditions and were used in all subsequent studies.

In Vitro Validation

The relative contrast decrease calculated from the CT images over time can be directly related to the concentration of iohexol in the explanted millirods at each time point. The correlation between these two modes of analysis was excellent in the *in vitro* gelatin system, as shown in Figure 3. The largest deviation between CT and UV-Vis data was 12%. Figure 3 insert shows linear correlation ($R^2 = 0.99$) of both analysis methods. This result proves conclusively that CT is capable of accurately determining the concentration of an active agent in a model system. Furthermore, it should be noted that the study was performed in duplicate ($n = 2$) with excellent data reproducibility (see error bars in Figure 3).

Table 1. Dependence of CT Sensitivity Limits on Image Acquistion Parameters

mAs	kVp	ΔZ (mm)	Sensitivity (mg/mL Iohexol)
600	120	1	0.21
400	120	1	0.23
200	120	1	0.30
400	140	1	0.24
400	90	1	0.22
600	120	2.5	0.18

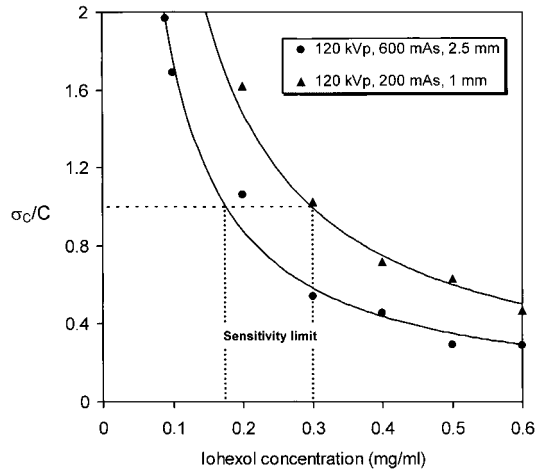

Figure 2. Determination of sensitivity cutoff for iohexol. Shown are plots from two image acquisition conditions exhibiting high (2.5-mm slice thickness, 120 kVp, 600 mAs) and low sensitivity (1 mm, 120 kVp, 200 mAs) with cutoff values at 0.18 and 0.30 mg/ml iohexol, respectively.

The relationship between iohexol concentration and CT intensity in Houndsfield units (which is reflective of the X-ray attenuation by iodine) was also found to be linear, as expected. A plot of CT intensity versus iohexol concentration in the implants was constructed based on the experimental

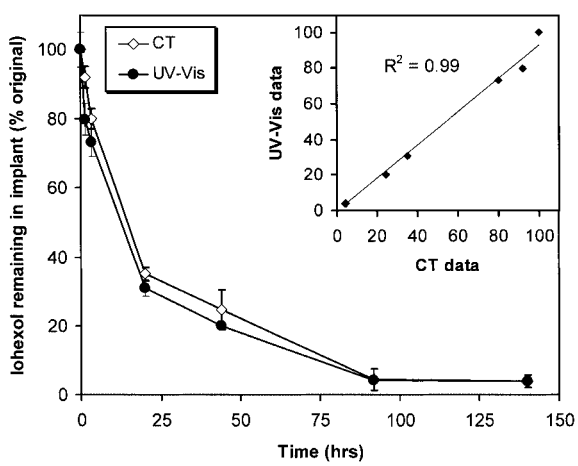

Figure 3. Comparison of iohexol release profiles in gelatin gels from CT method and UV-Vis analysis. Figure 3 insert shows the linear correlation of the two methods.

data. The slope for this relationship is 8.46 HU/(mg/mL). This value was used in the following *in vivo* studies to convert the image data to iohexol concentration.

Respiratory Motion Correction and Validation of CT *In Vivo*

The validity of the CT method was tested *in vivo* by directly monitoring the release of iohexol in rabbit livers at discrete time points. Figure 4 shows two CT slices of the same iohexol implant in a rabbit liver taken before and after sacrifice. It is evident that the respiratory motion plays a significant role in the quantitative image analysis at the current rotation time (1.5 s) chosen for this study. Iohexol concentrations calculated from images taken after sacrifice (no motion) were significantly higher than the concentrations calculated from breathing animals (Figure 5). When plotted against each other, the slope of a line fit to this data using linear regression was 1.4 ± 0.2. We used this value as the correction factor to calculate the *in vivo* release data from moving, breathing rabbits. This correction factor was further validated during ongoing experiments with excellent results in multiple rabbits. The correction is necessary to improve the accuracy of concentration measurement in live rabbits but will vary depending on the experimental conditions

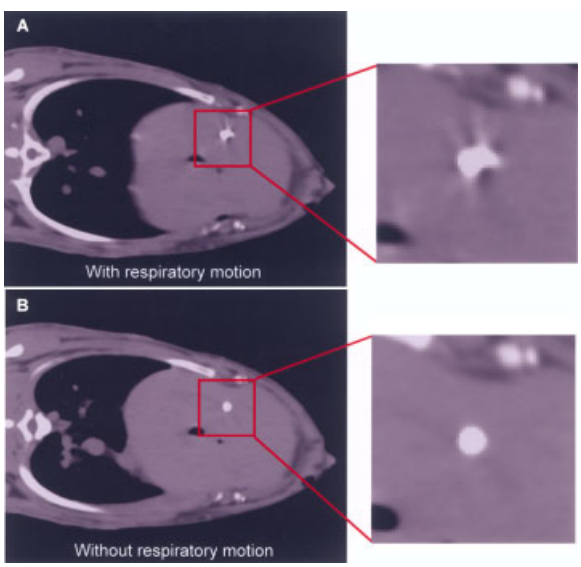

Figure 4. CT images with and without respiratory motion artifact. (A) A representative cross-sectional slice of the millirod in a live animal; (b) the slice following animal sacrifice.

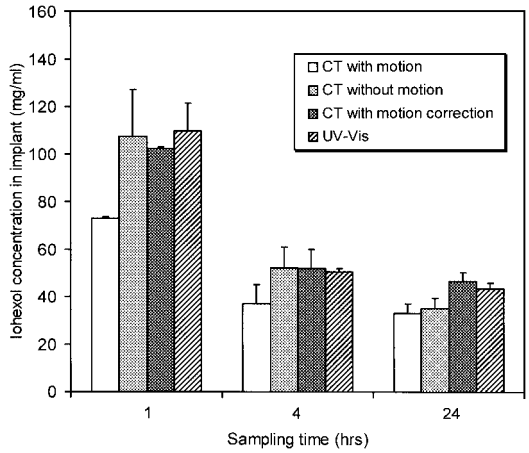

Figure 5. Comparison of four different analysis methods of iohexol release. Shown are CT data before and after motion correction, CT data without motion (following sacrifice), and UV-Vis analysis of explanted millirod.

(e.g., the breathing rate of the animal, and CT rotation time).

Figure 5 compares the iohexol concentrations obtained from four different analysis methods. The reduction in signal due to the motion blurring is apparent when comparing the CT data before correction to the other two analysis methods (CT without motion and UV-Vis analysis). The percent difference between uncorrected CT concentration values and UV-Vis data was 36, 26, 23% for samples at 1, 4, and 24 h, respectively. No statistically significant differences were observed between the CT (after motion correction) and UV-Vis values of extracted iohexol (based on a two-tailed, unpaired Student's *t*-test), validating the CT method *in vivo* and applicability of the correction factor. The percent errors (when treating the UV-Vis data as standard) were reduced by the correction to 6.8, 2.9, and 7.1% for samples at 1, 4, and 24 h, respectively.

DISCUSSION

Selection of Millirod Implant

The chief requirements for a drug delivery system appropriate for the current studies were a rapid release of the agent at a reproducible rate, and sufficient but modulated X-ray attenuation that was clearly visible but did not saturate the signal (maximum limit 4095 HU). The latter is quite important because if an intensity of the contrast were too great, information at the upper range

would be lost. Implants containing 10% iohexol and 30% glucose met the above requirements (2460 HU, $t_{1/2} = 10.1 \pm 1.2$ h) and were chosen for the gelatin gel and animal studies.

CT Optimization and Sensitivity

The sensitivity limit of CT is highly dependent on image noise and can be optimized by maximizing the signal to noise ratio. The image acquisition parameters that play a crucial role in this effect are the mAs, kVp, and slice thickness. The mAs is directly related to the number of photons emitted in an X-ray beam, and therefore it is inversely correlated to the noise of an image. The kVp affects the number of photons as well as the energy of the X-ray beam. Higher energy X-rays penetrate an object to a greater degree, while lower energy X-rays are attenuated more.[9,10] Increasing the energy of the beam, thus, increases the amount of signal reaching the detector, and thus increases the sensitivity. The slice thickness, which is affected by beam collimation, is also an important factor in the CT signal. Narrowing the collimation reduces the voxel size, thus decreasing the number of photons per voxel. This leads to an increase in quantum noise. In our application, it is important to achieve a maximum sensitivity limit without severely compromising resolution. Because a trade-off exists between the two, the optimization studies were a necessary step to determine the optimal parameter combination (e.g., 600 mAs, 120 kVp, 1 mm, as shown in Table 1).

Correction of Respiratory Motion in CT Monitoring of Iohexol Release

Gelatin gel provides an excellent *in vitro* model for CT validation because its high aqueous content (90%) and background X-ray attenuation (40 HU) are both similar to liver tissue. However, the gelatin model differs from a physiological system in one important aspect—motion. This motion artifact was quite evident in the rabbit model, even through qualitative examination of images of the implants in rabbits before and after sacrifice (Figure 4). The quantitative evaluation of these CT images confirmed the severity of this effect, and substantiated the fact that respiratory motion at a long rotation time (1.5 s) reduces the X-ray attenuation signal by a factor of 1.4. The effect is a result of object blurring on the image, particularly for small, bright objects (such as a 1.64 mm cross-section of the implant). Similar motion effects have been reported previously in another quantitative CT application—coronary calcium scoring.[16] The correction factor accounting for respiratory motion was applied to the data obtained from living rabbits and compared to data from UV-Vis. The corrected CT data approximated the actual iohexol concentration significantly better than prior to the correction (Figure 5). Other possible corrections for this artifact include a shorter rotation time and retrospective respiratory gating, both of which are currently under investigation in our laboratory.

Potential Limitations of CT in Drug Monitoring

Despite its vast promise, there are several issues that need to be addressed before the CT method can be reliably used for more in depth pharmacokinetic analysis. The primary issue involves applicability of the technique to therapeutic drugs, which are limited to chemicals containing a heavy element that will attenuate X-rays. Fortunately, there are currently 25 platinum-containing anticancer agents ($\mu_{m(\mathrm{Pt})} = 8.73$ cm^2/g at 80 keV) in clinical trials, and four have been approved for clinical use.[17] Thus, the CT method is directly applicable for studying the local pharmacokinetics of clinically used drugs, such as carboplatin and cisplatin. For most other drugs, covalent attachment of a heavy (but not radioactive) element may be necessary to generate CT contrast. However, special precaution needs to be taken to ensure the addition of such an element does not affect the drug pharmacokinetics and mechanism of action.

Another concern, which we have touched upon in this work, is the respiratory motion artifact. The correction factor used in this work is an interim solution to a crucial issue affecting the accuracy of the quantitative data as well as the sensitivity of the method. The tradeoff between longer scan times to improve sensitivity and motion reduction to prevent artifact requires further investigation, particularly for future application of the method in examining tissue penetration and distribution of a drug in animals as well as in humans.

CONCLUSIONS

The excellent *in vitro* and *in vivo* validation results conclusively demonstrate the feasibility of computed tomography in noninvasive drug monitoring. The CT method has a number of

unique advantages in local pharmacokinetic studies. Primarily, CT has a superb combination of sensitivity and resolution compared to other imagining modalities. Moreover, CT allows a rapid collection of many high-resolution images (less than 20 s per animal scan) and can minimize the variability of release kinetics due to long scanning time (e.g., MRI scans often take significantly longer). Furthermore, it eliminates the need for extensive tissue collection and requires fewer animals than more traditional pharmacokinetic analysis. This noninvasive nature, in turn, minimizes animal variability. Current work is in progress to apply this method in characterizing and comparing the release kinetics of iohexol in normal and thermally ablated liver tissue *in vivo*.

ACKNOWLEDGMENTS

The authors would like to thank Les Ciancibello for his help with the CT image acquisition, and Dr. Uri Shreter from Philips Medical Systems for helpful discussions. Funding for this project was provided by the Whitaker Foundation (RG 99-0342) and National Institutes of Health (R21 CA93993).

REFERENCES

1. Benet LZ, Kroetz DL, Sheiner LB. 1996. Pharmacokinetics: The dynamics of drug absorption, distribution, and elimination. In: Hardman JG, Limbird LE, editors. Goodman & Gilman's The pharmacological basis of therapeutics, 9th ed. New York: McGraw-Hill. pp 3–27.
2. Singh M, Waluch V. 2000. Physics and instrumentation for imaging in-vivo drug distribution. Adv Drug Del Rev 41(1):7–20.
3. Wolf W. 2000. Introduction and overview of noninvasive drug monitoring. Adv Drug Deliv Rev 41(1):1–5.
4. Bhatnagar A, Hustinx R, Alavi A. 2000. Nuclear imaging methods for non-invasive drug monitoring. Adv Drug Del Rev 41(1):41–54.
5. Taylor J. 2000. Evolution from empirical dynamic contrast-enhanced magnetic resonance imaging to pharmacokinetic MRI. Adv Drug Del Rev 41(1):91–110.
6. Saleem A. 2000. In vivo monitoring of drugs using radiotracer techniques. Adv Drug Del Rev 41(1): 21–39.
7. Griffiths JR, Glickson JD. 2000. Monitoring pharmacokinetics of anticancer drugs: Non-invasive investigation using magnetic resonance spectroscopy. Adv Drug Del Rev 41(1):75–89.
8. Dowsett DJ, Kenny PA, Johnston RE. 1998. The physics of diagnostic imaging. London: Chapman & Hall Medical. pp 107–127.
9. Bushberg JT, Seibert JA, Leidholdt EMJ, Boone JM. 1994. The essential physics of medical imaging. Baltimore: Williams & Wilkins. pp 239–290.
10. Curry TS, Dowdey JE, Murry RC. 1990. Christensen's physics of diagnostic radiology, 4th ed. Philadelphia: Lippincott Williams & Wilkins. pp 70–87.
11. Hubbell JH, Scofield JH. 1988. X-ray attenuation cross sections for energies 100 eV to 100 keV and elements $Z = 1$ to $Z = 92$. Atomic Data and Nucl Data Tables 38:1.
12. Qian F, Szymanski A, Gao J. 2001. Fabrication and characterization of controlled release poly(D,L-lactide-*co*-glycolide) millirods. J Biomed Mater Res 55(4):512–522.
13. Lazebnik RS, Lancaster TL, Breen MS, Lewin JS, Wilson DL. 2001. Volume registration using needle paths and point landmarks for evaluation of interventional MRI treatments. IEEE Transact Med Imag, submitted.
14. Lazebnik RS, Lancaster TL, Breen MS, Nour SG, Lewin JS, Wilson DL. 2002. Volume registration of interventional MRI data using needle paths and point landmarks. Proceedings of SPIE Medical Imaging 2002: Visualization, display, and image-guided procedures. SPIE, Vol. 4681, pp 39–46, 2002.
15. Salem KA, Szymanski-Exner A, Lazebnik RE, Breen MS, Gao J, Wilson DL. 2002. X-ray computed tomography methods for *in vivo* evaluation of local drug release systems. IEEE-Transact Med Imag in press.
16. Brown SJ, Hayball MP, Coulden RAR. 2000. Impact of motion artifact on the measurement of coronary calcium score. Br J Radiol 73:956–962.
17. Lebwohl D, Canetta R. 1998. Clinical development of platinum complexes in cancer therapy: A historical perspective and an update. Eur J Cancer 34(10): 1522–1534.